



CHARLES UNIVERSITY
Faculty of Pharmacy
in Hradec Králové

**Effect of Sphingosine Phosphorylcholine
on the *stratum corneum* Permeability**

Hradec Králové 2020

Khalied Mahrous Farid Bataalla

Statement of Originality

I declare that this diploma thesis is my own personal work and that I worked on it on my own. All literature and other resources that I used are listed in the references list and are properly cited.

Hradec Králové

Khalied Mahrous Farid Bataalla

2020

Acknowledgments

I would like to express my deepest appreciation to my supervisor PharmDr. Andrej Kováčik, Ph.D. for his guidance throughout my thesis. His patience and immense knowledge made this project a success. I would also like to thank to my consultant Dr. Georgios Paraskevopoulos, PhD., Mgr. Anna Nováčková, and other members of *Skin Barrier Research Group*, and the head of research group, prof. PharmDr. Kateřina Vávrová, Ph.D. I would like to thank for the financial support (GAČR 19-09135J and SVV 260547).

Table of Content

| | |
|--|----|
| Abstrakt | 6 |
| Abstract | 7 |
| Abbreviations | 8 |
| List of Figures and Tables | 10 |
| 1. Introduction..... | 11 |
| 1.1. Function of Human Skin | 11 |
| 1.2. Human Skin Composition | 11 |
| 1.3. Human Epidermis Composition | 12 |
| 1.4. Lipid Matrix of <i>stratum corneum</i> | 13 |
| 1.5. Ceramide Biosynthesis..... | 15 |
| 1.6. Organisation of Skin Lipids in <i>stratum corneum</i> | 16 |
| 1.7. Sphingomyelin, Sphingosine Phosphorylcholine and Skin Diseases..... | 18 |
| 2. Goal of Work | 21 |
| 3. Materials and Methods..... | 22 |
| 3.1. Chemicals | 22 |
| 3.2. Human Skin..... | 22 |
| 3.3. Human SC Isolation | 22 |
| 3.4. Sample Preparation | 22 |
| 3.5. High Performance Thin Layer Chromatography (HPTLC) | 23 |
| 3.6. Permeation Experiments | 24 |
| 3.7. Donor Samples for Permeation Studies | 24 |
| 3.8. TEWL Measurement | 24 |
| 3.9. Measurement of Electric Impedance..... | 25 |
| 3.10. High performance liquid chromatography (HPLC) of IND and TH..... | 25 |
| 3.11. Evaluation of Permeation Data..... | 25 |
| 3.12. Fourier-Transform Infrared (FTIR) Spectroscopy | 26 |
| 4. Results and Discussion | 27 |
| 4.1. TEWL..... | 27 |
| 4.2. Electric Impedance..... | 28 |
| 4.3. Permeability to TH and IND | 30 |
| 4.4. FTIR Spectroscopy..... | 32 |

| | |
|---|----|
| 4.5. High Performance Thin Layer Chromatography | 33 |
| 5. Conclusions..... | 35 |
| 6. References..... | 36 |

Abstrakt

Univerzita Karlova

Farmaceutická fakulta v Hradec Králové

Katedra farmaceutické technologie

Kandidát: **Khalied Mahrous Farid Bataalla**

Školitel: **PharmDr. Andrej Kováčik, Ph.D.**

Konzultant: **Dr. Georgios Paraskevopoulos, PhD.**

Název diplomové práce: **Effect of Sphingosine Phosphorylcholine on the *stratum corneum* Permeability**

Sfingosin-fosforylcholin (SPC) je sfingolipid, který patří do velké rodiny lysolipidů. Tato sloučenina vzniká z prekursoru ceramidů, sfingomyelinu, a to působením enzymu sfingomyelindeacylázy. Tato sloučenina je tvořena sfingoidní bází (např. sfingosinu) a fosforylcholinové jednotky, které jsou spojeny přes hydroxylovou funkční skupinu. V této práci jsme studovali vliv SPC na bariérovou funkci a mikrostrukturu (organizaci) modelových membrán *stratum corneum* (SC). K tomuto hodnocení jsme použili čtyři parametry permeability: elektrickou impedanci, trans-epidermální ztrátu vody (TEWL), flux (tok) indometacinu a flux teofylinu. Z výsledků permeačních experimentů jsme zjistili, že přidavek (aplikace) SPC statisticky zvyšuje propustnost SC pro vodu a ionty (zvýšené hodnoty TEWL a elektrické impedance). Tento trend jsme rovněž pozorovali u třetího (propustnost pro teofylin) a čtvrtého (permeabilita k indometacinu) parametru propustnosti. Negativní vliv SPC na SC bylo studováno pomocí biofyzikálních experimentů (infračervená spektroskopie, FTIR). V infračervených spektech modelů SC jsme pozorovali (bez statistických rozdílů) posun vibračního pásu methylenových valenčních symetrických vibrací do vyšších hodnot vlnočtů. Toto značí horší uspořádání lipidů v modelech SC. Tato práce by mohla přispět k objasnění významu lysolipidů ve zdravém i nemocném SC a také by mohla být nápomocná při pochopení významu změn hladin lipidů v patofyziologii kožní tkáně.

Abstract

Charles University

Faculty of Pharmacy in Hradec Králové

Department of pharmaceutical technology

Candidate: **Khalied Mahrous Farid Bataalla**

Supervisor: **PharmDr. Andrej Kováčik, Ph.D.**

Adviser: **Dr. Georgios Paraskevopoulos, PhD.**

Title of Diploma Thesis: **Effect of Sphingosine Phosphorylcholine on the *stratum corneum* Permeability**

Sphingosine phosphorylcholine (SPC) is a sphingolipid, which belongs to a lysolipid family. This compound, formed from ceramide precursor – sphingomyelin by the action of sphingomyelin deacylase, is composed of sphingoid base (*e.g.*, sphingosine) and phosphorylcholine moiety joined to a hydroxyl group. In this project, we studied how SPC influences the barrier function and microstructure of model *stratum corneum* (SC) membranes. Four permeability markers were used to study the permeability of SPC: electric impedance, trans-epidermal water loss (TEWL), flux of indomethacin and flux of theophylline. From this study we found out that the addition of SPC significantly increases the permeability to water and ions (increased values of TEWL and decreased values of electric impedance). This trend was also observed on third (permeability to theophylline) and fourth (permeability to indomethacin) permeation markers. The detrimental effect of SPC was also studied in biophysical experiments (infrared spectroscopy, FTIR). From methylene symmetric stretching of lipids in model SC membranes with an addition of SPC we observed (not significantly) the shift to higher wavenumbers, which suggest the less ordered chains of skin lipids in SC. This study could partially elucidate the role of lysolipids in some skin diseases and be helpful to clarify the understanding the lipid changes in pathology of the skin tissue.

Abbreviations

| | |
|------------|---|
| AD | atopic dermatitis |
| ATR-FTIR | attenuated total reflection Fourier-transform infrared spectroscopy |
| BmSM | sphingomyelin from bovine milk |
| Cer | ceramide |
| Chol | cholesterol |
| CholS | sodium cholesteryl sulfate |
| EtOH | ethanol |
| eSM | sphingomyelin from chicken egg |
| FFA | free fatty acid |
| GlcCer | glycosylceramides |
| GlcCer'ase | β -glucocerebrosidase |
| GD | Gaucher disease |
| HPLC | high-performance liquid chromatography |
| HPTLC | high-performance thin layer chromatography |
| IND | indomethacin |
| LPP | long periodicity phase |
| Mw | molecular weight |
| PG | propylene glycol |
| PBS | phosphate buffered saline |
| SM | sphingomyelin |
| SC | stratum corneum |
| SEM | standard error of mean |
| SMase | sphingomyelinase |

| | |
|-------|--|
| SPC | sphingosine phosphorylcholine |
| SPP | short periodicity phase |
| TH | theophylline |
| TEWL | trans-epidermal water loss |
| NADPH | nicotinamide adenine dinucleotide phosphate hydrogen |

List of Figures and Tables

Figures

- Figure 1** Structure of human skin
- Figure 2** Structure of human epidermis
- Figure 3** Structure of cholesterol, free fatty acids and skin ceramides in the skin barrier
- Figure 4** Model structure of skin Cer
- Figure 5** Skin Cer biosynthesis in the endoplasmatic reticulum
- Figure 6** Lamellar (short and long periodicity phase) and lateral (orthorhombic, hexagonal, and liquid) organisation of the SC lipid membranes (lamellae)
- Figure 7** Skin Cer conformations (hairpin and extended conformation)
- Figure 8** Sphingolipid metabolism in epidermis discovered in atopic dermatitis
- Figure 9** Effect of SPC on the SC permeability I.
- Figure 10** Effect of SPC on the SC permeability II.
- Figure 11** Effect of SPC on the SC permeability III.
- Figure 12** Effect of SPC on the SC permeability IV.
- Figure 13** FTIR spectroscopy and lipid chain order of model SC samples at physiological temperature of 32°C

Tables

- Table 1** Skin Cer (key components of SC) shorthand nomenclature created by Motta *et al.*

1. Introduction

1.1. Function of Human Skin

Skin is the largest organ of the human body; its function is to protect the skin against physical and chemical factors such as chemicals and unwanted substances. Skin helps to control body temperature and to maintain moisture; it prevents the water loss. Human skin prevents the entry of bacteria, viruses and pollution into the body. Skin tissue involves in the synthesis of vitamin D. The human skin as a complex organ has many functions, such as the excretion of unwanted water (sweating by sweat glands), respiration or immunological function. Moreover, the skin protects against trauma and UV rays, etc.¹⁻⁴

1.2. Human Skin Composition

The human skin consists of three functionally different layers, *i.e.*, epidermis, dermis and hypodermis, as shown in **Figure 1**.

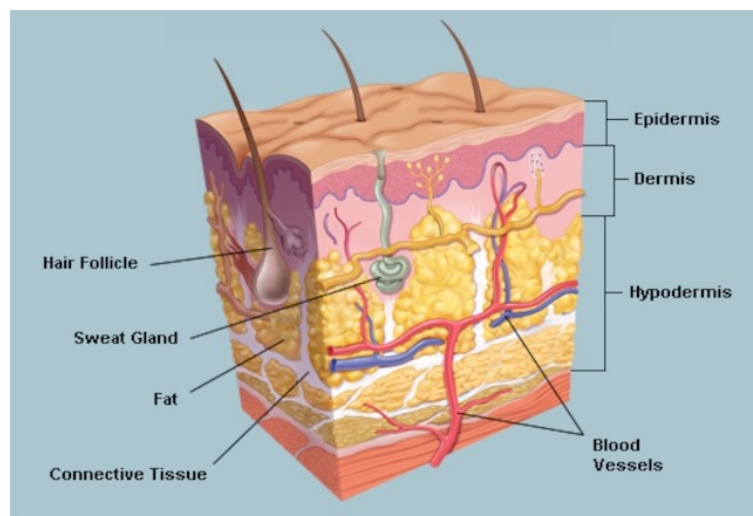


Figure 1. Structure of human skin, *i.e.*, skin layers (epidermis, dermis, and hypodermis).⁵ There in the figure, some skin derivatives (sweat gland, hair follicles), and blood vessels are depicted.

Hypodermis (fat layer) is the innermost layer of the skin; it protects the body from cold, heat and plays a role as a storage area for energy. This layer, composed of adipocytes filled with triacylglycerols (triglycerides), plays an important role in mechanical barrier of the human body, *i.e.*, it protects the muscles and other tissues (organs) against the mechanical stressor factors.¹ **Dermis** is the thicker layer of the skin located below epidermis which contains sweat glands, hair follicles, blood vessels and nerve endings. The main part of this layer is a mixture

of two basic components – **collagen** and **elastin**. In the healthy skin, there is a huge amount of collagen subclasses. These filaments along with elastin give the strength, elasticity, flexibility and tonus.¹ The main component of these filaments are amino acids, for instance hydroxylated amino acid hydroxy-Proline (OH-Pro). In this layer, many skin derivatives can be found. To the most important appendages we can classify the glands (sweat glands for excretion/respiration and sebaceous glands for the production of sebum), then hair follicles and nails.

Epidermis is the outermost layer of the skin, composed of keratinocytes (skin cells), which form from 4 to 5 layers^{6, 7} (**Figure 2**). The most important epidermal layers are *stratum basale*, *stratum spinosum*, *stratum granulosum* and the outermost epidermal layer, *i.e.*, *stratum corneum*. In addition, the *stratum lucidum* is counted to the epidermal layers (see below).

1.3. Human Epidermis Composition

In this chapter, the epidermal layers and their structure and function are described.⁸ Epidermal layers (**Figure 2**) are:

- ***Stratum basale***. This layer is the deepest layer of the epidermis. There, in *stratum basale*, the cells are linked with the dermis by collagen fibres links.
- ***Stratum spinosum***. The cells in this epidermal layer are joined by desmosomes. The desmosome strength the bond between the cells. *Stratum spinosum* consists of between 8 to 10 layers of keratinocytes.
- ***Stratum granulosum***. In this layer, skin cells produce a large quantity of the protein keratin and keratohyalin.
- ***Stratum lucidum***. This layer is localized between the *stratum granulosum* and the uppermost layer of the skin, the *stratum corneum*. This layer is only found in thick skin.
- ***Stratum corneum* (SC)**. This layer is the outermost layer of human epidermis, it is composed of 20 to 30 layers of dead keratinocytes, well known as corneocytes. These cells do not contain any compartments and nuclei. Corneocytes plus intercellular skin lipids (lipid matrix; see below) play an essential role in the proper skin barrier, *i.e.*, the prevention the water loss and entering of unwanted substances.^{3, 9}

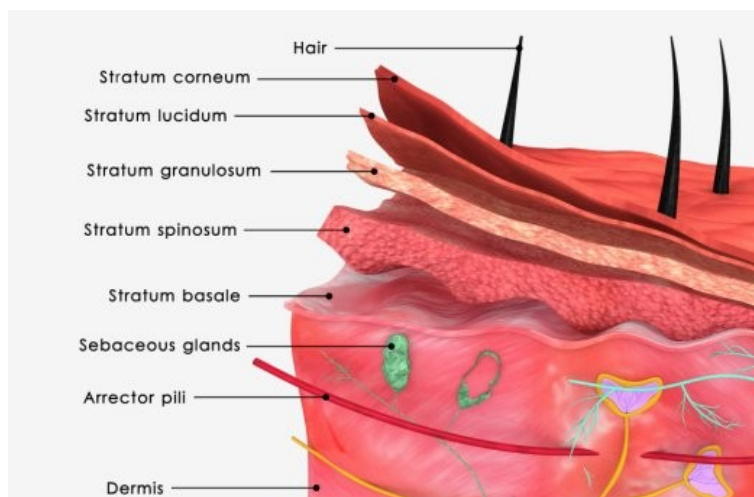


Figure 2. Structure of human epidermis, *i.e.*, stratum basale, stratum spinosum, stratum granulosum, stratum lucidum, and stratum corneum.¹⁰

1.4. Lipid Matrix of *stratum corneum*

Lipid matrix of SC consists of a molar ratio (1:1:1 mol)^{6, 11, 12} of three classes of skin lipids, *i.e.*, **cholesterol (Chol)**, **free fatty acids (FFA)**, and **ceramides (Cer)**¹³ as shown in **Figure 3**.

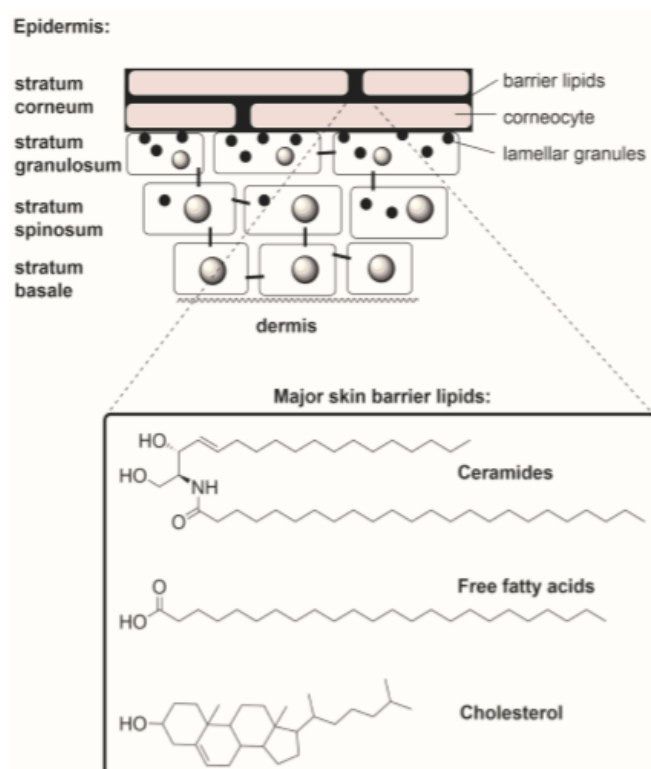


Figure 3. Structure of cholesterol, free fatty acids and skin ceramides in the skin barrier.⁶

Chol is a steroid (sterol type) molecule, which was found naturally in body tissues, in skin care products it helps the rebuild or repair of skin and maintains its flexibility.^{6, 14, 15} FFA is a mixture of saturated, unbranched fatty acids with different chain length (mostly C16-C24). The most abundant FFA in the SC lipid matrix is lignoceric acid (C24) and behenic acid (C22).^{7, 9, 16}

Cer are sphingolipids composed of sphingosine (sphingoid base) and fatty acid^{6, 7, 17, 18} (as an acyl chain), which is linked via amide bond as shown in **Figure 4** (see below). Skin Cer occur in the skin naturally, they form approximately 50% of skin lipid content. Cer molecule is composed of two parts:

- **sphingoid base** (usually 18 carbons) – amino-alcohol with chiral carbons. In the healthy human epidermis, Cer molecules contain either sphingosine (with *trans*-double bond, S),¹⁹ or dihydrosphingosine²⁰ (*trans*-double bond in the chain backbone is missing, dS), or phytosphingosine²¹ (with an additional hydroxyl group in C-4 position), or 6-hydroxysphingosine (with *trans*-double bond in C-4 and a hydroxyl group in C-6 position).^{17, 22}
- **fatty acid acyl** – unsaturated, unbranched carbon chain. The acyl can be non-hydroxylated (N), or hydroxylated in position alfa- (A)²³ or omega- (O).²⁴⁻²⁶

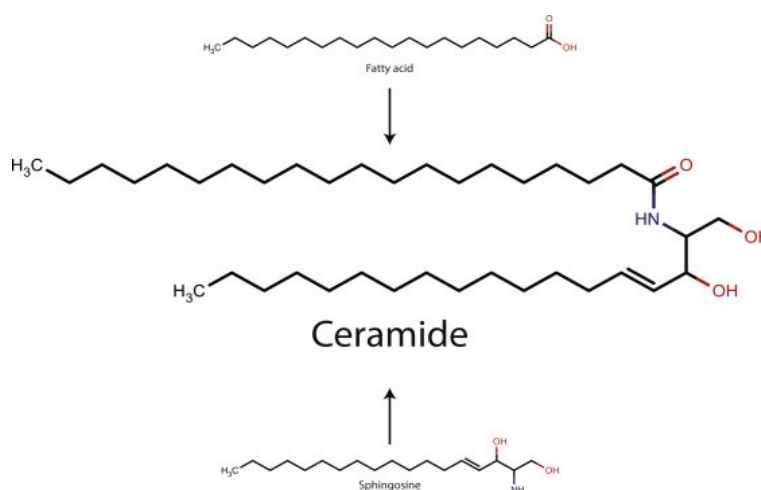


Figure 4. Model structure of skin Cer, i.e., sphingoid base (sphingosine) and fatty acid acyl derived from fatty acid with 20C.¹³

There are huge possibilities for Cer classification. In this work, a nomenclature developed by **Motta et al.**²⁷ is used (acronyms for sphingoid bases and acyls are in brackets above). By the combination of different types of sphingid bases and fatty acid acyls, a wide collection of 15 subclasses is known (**Table 1**). Beside the free Cer, some of omega-

hydroxylated Cer are covalently bound to corneocyte proteins, and they are called as protein bound Cer. Covalently bound Cer play a crucial role in the **corneocyte lipid envelope** formation and stabilization.²⁸⁻³⁰

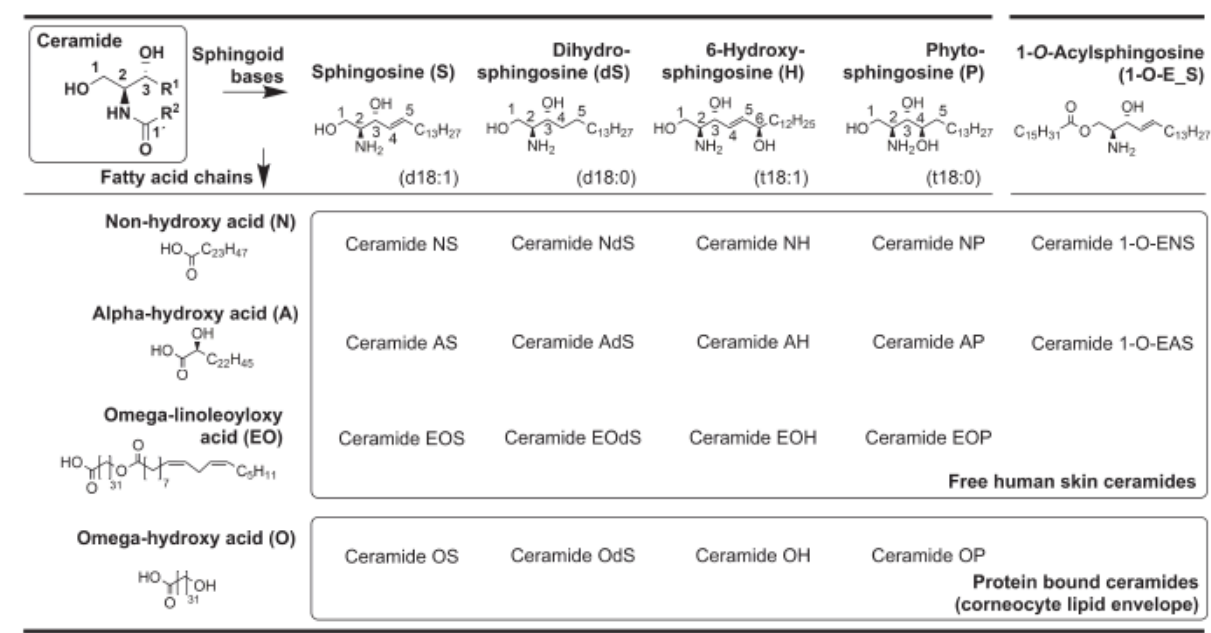


Table 1. Skin Cer (key components of SC) shorthand nomenclature created by Motta et al.²⁷ (13)

The functions of the skin Cer is the following: prevention the water loss from the skin, they play an important role as a protective barrier against harm substances that can penetrate through the skin.^{6, 31, 32}

1.5. Ceramide Biosynthesis

The skin Cer *de novo* synthesis starts in endoplasmatic reticulum. First step of this synthesis is a condensation of amino acid L-serine and palmitoylCoA to obtain 3-ketodihydro-sphingosine, known as **3-ketosphinganine**. Next, 3-ketodihydro-sphingosine is reduced (keto-group is reduced to hydroxyl-group) to **dihydro-sphingosine** (dS). Some groups of *Cer synthase* enzyme act an important role in the next step, *i.e.*, the **dihydroceramide** (dihydro-sphingosine-based Cer, dS-Cer) is formed (see **Figure 5**). This molecule serves as a precursor for other skin Cer subclasses.^{8, 33-35}

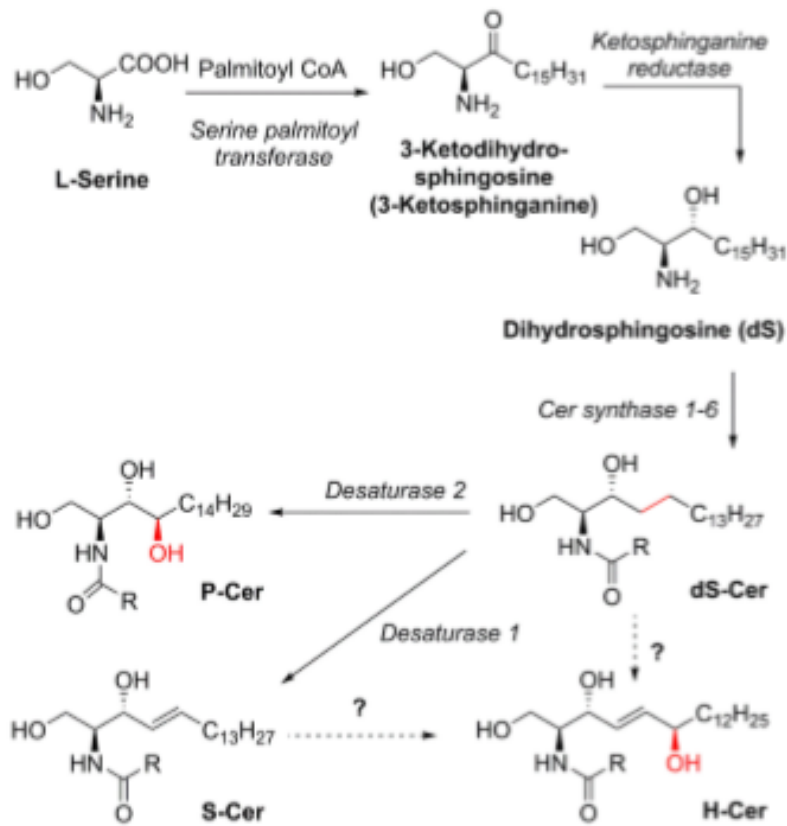


Figure 5. Skin Cer biosynthesis in the endoplasmatic reticulum. From the L-Serine and palmitoylCo A, 3-ketosphinganine is formed. From this molecule, the dihydrosphingosine, dihydroceramide, and other skin Cer are formed.¹⁷

From dihydroceramide (by the action of *desaturase*), a sphingosine-based (S-Cer), or phytosphingosine-based Cer (**phytoceramide**, P-Cer) are formed. However, the biosynthesis of 6-hydroxysphingosine-based Cer (**6-hydroxyceramide**, H-Cer) is still unknown.³⁶ Probably, some hydroxylases incorporate an additional hydroxyl group into C-6 position.¹⁷ The skin Cer synthesis *de novo* is depicted in **Figure 5**.

1.6. Organisation of Skin Lipids in *stratum corneum*

In contrast to phospholipids (normally form the cell bilayers), Cer bear a very small polar (hydrophilic) head. In addition, the Cer molecule contains two long saturated hydrophobic chains. In the SC, Cer molecules among with FFA and Chol and other lipids form lipid lamellae, *i.e.*, multilamellar lipid membranes.³⁷⁻⁴⁰ In the healthy SC, lipids are lamellar organized in lamellar system called as **long periodicity phase** (LPP) with a replicate length (repeat distance; *d*) of 11.9–13.1 nm.^{40,41} This lamellar phase was discovered by electron microscopy⁴² and later

on by X-ray diffraction.^{28,43} The presence of LPP, determined by ultralong-chain Cer (Cer EO-type), is essential for the proper skin barrier function, *e.g.*, to prevent the water loss. In addition, majority of the studies had reported the occurrence of **short periodicity phase (SPP)** with a replicate length of 5.3-6.4 nm.^{39, 43-46} A **phase of separated Chol** ($d = 3.4$ nm)^{14, 15, 47} has been also found in the healthy SC lipid matrix. The phase separation of Chol is physiological, but still unknown.

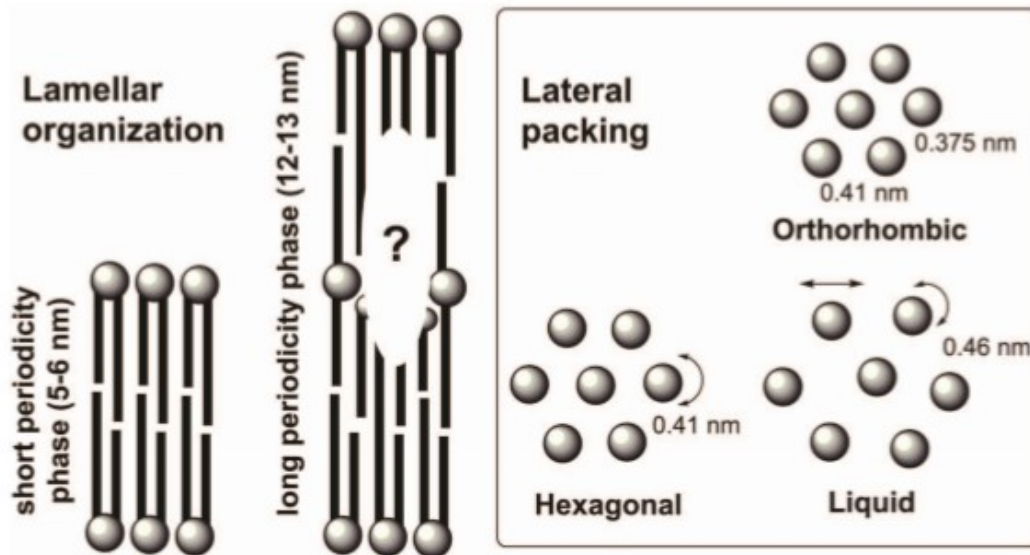


Figure 6. Lamellar (short and long periodicity phase) and lateral (orthorhombic, hexagonal, and liquid) organisation of the SC lipid membranes (lamellae).⁶

The lateral organisation of the skin lipids (mainly the CH₂ chains in Cer and FFA) can be in **orthorhombic** subcell (**Figure 6**), which is compacted with extremely limited motional freedom. In this subcell, the all-*trans* conformers (*zik-zak*) are predominant. Nevertheless, certain lipids are organised in a **hexagonal** subcell, which is typical by more significant rotational freedom. Small lipid part in lipid matrix is **fluid** (liquid subcell). In hexagonal subcell, the number of less ordered *gauche* conformers is present. In the fluid subcell, formed approximately by 1%, only the disordered *gauche* conformers are present^{38, 48-51}

Due to the multilamellar organisation of lipids in the SC, the extended conformation and the hairpin conformation (with the both chains pointing to the identical direction) of Cer are theoretically able to be achieved. However, the extended conformation is not so familiar in the biological membrane, but it could be favourable for the SC as it could decrease the packing force of ceramide (as they have tiny cross-sectional polar head comparing to the other chains), as well joins the lipid lamellae and to stop the permeable boundaries.⁶

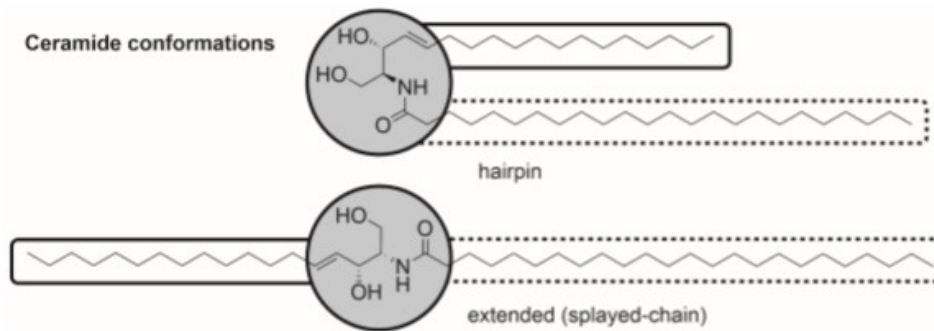


Figure 7. Skin Cer conformations (hairpin and extended conformation); in the figure, Cer NH (i.e., *N*-lignoceroyl 6-hydroxysphingosine) is depicted.⁶

1.7. Sphingomyelin, Sphingosine Phosphorylcholine and Skin Diseases

Sphingomyelin (SM) is transformed to phosphoryl choline and Cer by the enzyme sphingomyelinase (SMase).⁵² It consists of Cer unit with phosphoryl choline moiety attached to position 1. SM is synthesized in endoplasmatic reticulum. Around 90% of SM synthesis occurs in liver, and it also occurs in plasma membrane, which is the important in forming SM from recycled Cer. In diseases, such as Niemann–Pick disease and atopic dermatitis, shortage of sphingomyelinase (SMase) diminish the skin barrier healing after any damage which is resulted by mutation in SMPD1 gene. This leads to massive decrease in SMase activity. The character of SMase in leading to diminish skin barrier is not fully clear. To determine the result of decreased SMase activity is also not fully clear. According to Schmuth *et al.*,⁵² they applied SMase inhibitor to the skin of hairless mice, which results in decreased 4-fold accumulation of SM in the murine SC after an acute barrier disturbance. The resulted new ratio of SM/Cer was responsible for the changed skin barrier function. Deficiency in SM biosynthesis results in change in the normal physiology of the cell and the organism.⁵²

Sphingosine phosphorylcholine (SPC) is sphingolipid, which among the glucosyl sphingosine belong to a lysolipid family. As shown in (**Figure 8**), SPC is formed from sphingomyelin by the sphingomyelin deacylase. SPC is composed of sphingoid base (e.g., sphingosine) and phosphorylcholine moiety, joined to a hydroxyl-group. This molecule has been recognised in normal blood plasma, SPC are alike in structure of sphingosine-1-phosphate and lyso-phosphatidylcholine (**Figure 8**). SPC has some roles in biological processes, such as promotion the DNA synthesis, cell growth stimulation, prevent apoptosis, inhibition of cell proliferation, activation of actin stress fibre formation and calcium release from the

endoplasmatic reticulum in various cells types. Its released when the platelet is activated and is found in concentration around 50 to 130 nM in plasma. SPC activates various signals, it stimulates the development of many cancer types, it progresses the invasion of breast cancer cells, it decreases the level of organ dysfunction and it has strong anti-inflammatory properties.⁵³⁻⁵⁵

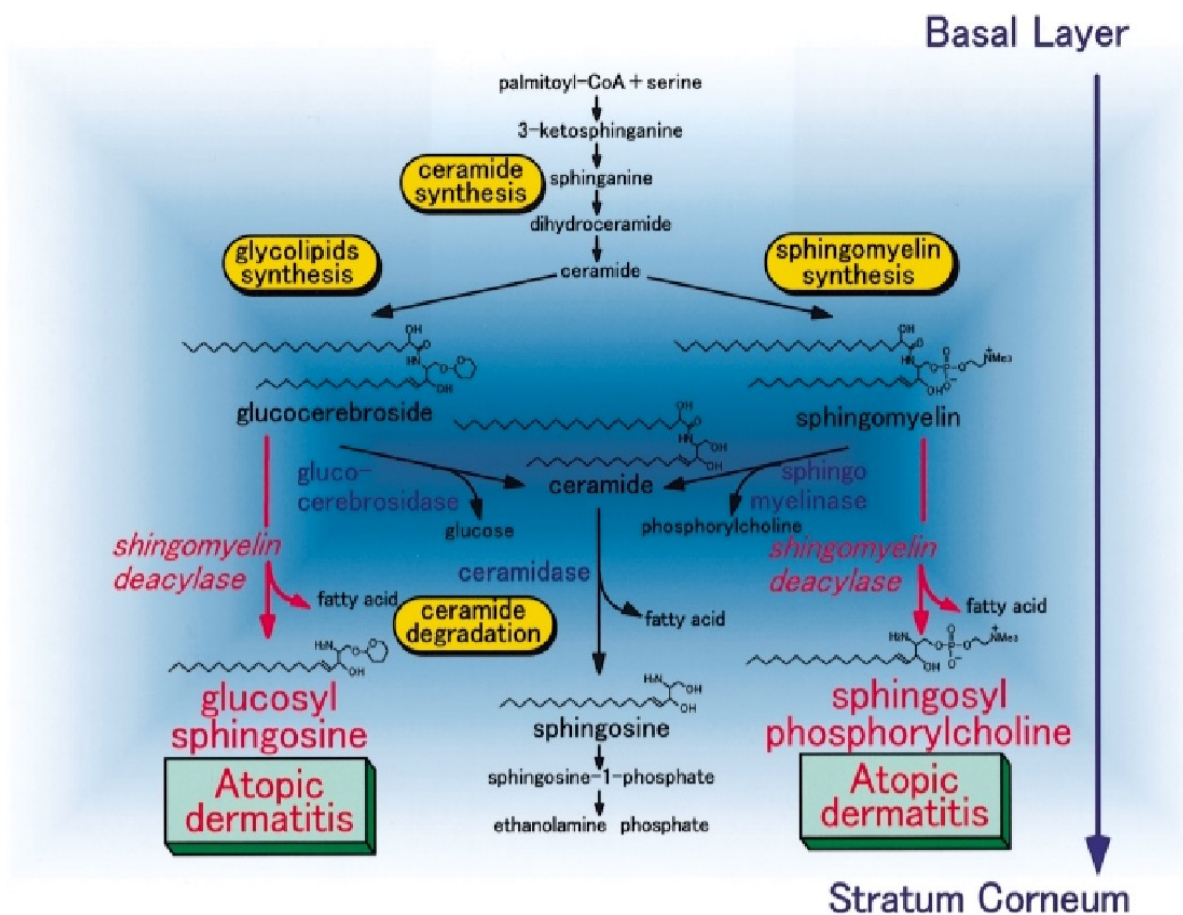


Figure 8. Sphingolipid metabolism in epidermis discovered in atopic dermatitis⁵⁶

These biological activities take place as well in several different types of cells located in the skin such as melanocytes, fibroblasts, keratinocytes and endothelial cells. SPC also plays an essential role in the activation of mitogen associated protein kinase (MAP). In addition, SPC increases the effect on wound healing after the application onto the skin *in vivo*.^{53, 56}

In many patients with skin disorders such as atopic dermatitis lower amounts of Cer, in comparison to healthy skin, has been detected. Interestingly, the higher levels of lysolipids (especially SPC) was found. However, there has been no abnormality of the enzymes used in Cer biosynthesis such as *serine palmitoyl transferase* long chain base subunits or *Cer synthase*.

In addition, it has been discovered that the enzyme *sphingomyelin deacylase* removes the *N*-acyl linkage of the sphingomyelin leading to formation of SPC. In extracellular application of SPC results in changed cell migration, cytoskeleton disarrangement, a fast increase in intracellular calcium and activates acetyl-choline sensitive potassium current in atrial myocytes.^{32, 53-55, 57, 58}

2. Goal of Work

The aim of my work was to study effect of Cer-precursor metabolite (SPC) on the **permeability and microstructure of the SC**. In this work, the human SC was isolated from the skin tissue, and then the permeability (**electric impedance, trans-epidermal water loss and flux of theophylline (TH) and flux of indomethacin (IND)**) and microstructure (**infrared spectroscopy**) have been investigated. The experimental part of this work is divided into following parts: materials and methods (chemicals and experimental procedure describing), results and discussion and conclusions.

3. Materials and Methods

3.1. Chemicals

Sphingosine phosphorylcholine (SPC) was purchased from Avanti Polar Lipids (Alabaster, USA). Theophylline (anhydrous; TH), indomethacin (anhydrous; IND), trypsin from porcine pancreas (1:250; powder), propylene glycol (PG), ethanol (EtOH) and other chemicals and solvents were purchased from Merck-Sigma-Aldrich Chemie GmbH (Schnelldorf, Germany). All solvents were analytical or HPLC grade.

3.2. Human Skin

The human skin was obtained from female patients who had undertaken plastic surgery (Private Surgery Departments SANUS Hradec Králové, Czech republic). In under 6 hours of the surgery, the subcutaneous fat layer was detached by a scalpel from the skin. The skin (epidermis + dermis) was removed with a paper tissue. The skin was then cleaned in a phosphate buffered saline at pH=7.4 (PBS solution, 10 mM buffer adjusted to 150 mM ionic strength containing 137 mM NaCl, 8 mM Na₂HPO₄·12H₂O, 2 mM NaH₂PO₄·2H₂O and 2.7 mM KCl) with 50 mg/L gentamicin for preservation. Then the clean and dried skin was stored at -20°C in the freezer.

3.3. Human SC Isolation

The isolation of the human SC was done by adjusting procedure described by Kligman and Christophers.⁵⁹ The frozen skin was gently warmed and dipped in water Millipore for 30 s at 60°C. The epidermis was carefully removed by tweezers. After that, epidermis was incubated overnight in a PBS solution (pH = 7.4) with 0.5% trypsin (the addition of trypsin enzyme is important for destruction of living layers of epidermis as only SC is needed for my experiment) at 32°C for 24 h. After that, the SC was washed couple of times in a Millipore water and once in acetone (to remove the rest of the surface lipids).

3.4. Sample Preparation

After the washing SC, tissue was applied onto the supporting filters. Note: use of supporting filters was used because of better manipulation with the tissue during the experiment; supported filters do not affect the permeability of SC. Afterwards, SC samples have been fitted in the

Teflon holders with circular diffusion area of 1 cm². Teflon holders with the samples have been installed into modified Franz diffusion cells. Franz diffusion cell composes of the donor and acceptor part. Acceptor compartment contains the shoulder (for sampling) and magnetic stirrer (for stirring). Franz cells have been put into the water bath (32°C) and kept at this temperature overnight. The next day, the TEWL and electric impedance of all the samples were measured. Afterwards, the 100 µL of 1% solution of SPC in propylene glycol/ethanol (7:3, v/v) was applied on each sample of SC.⁶⁰ In total, two types of samples were prepared: controls (SC + blank mixture of solvents) and SPC samples (SC + 1% solution of SPC in mixture of PG/EtOH). After the application of solvents/SPC solutions, the samples were equilibrated at 32°C (water bath) for 12 h. Next day, the solvents/1% solution were carefully removed, and the samples were washed with PBS buffer and dried with ear sticks. After that, samples were again equilibrated at same temperature overnight. Next, the permeation experiments (water loss, electric impedance and permeability to TH and IND) were performed, see below.

3.5. High Performance Thin Layer Chromatography (HPTLC)

In this study we aimed to determine the amount of SPC in SC after its application on the tissue. The isolates SC was first applied onto the supporting filter and put into Franz diffusion cells, *i.e.*, in the same way as samples for the permeation experiment. The tissues + supporting filters were incubated (= equilibrated) in water bath at 32°C for 3 hours, and after this time, the solution of lysolipid (SPC) in PG/EtOH was applied (same volume as for the permeation experiment). Next day, the samples were carefully washed with Millipore water and the diffusion area of 1 cm² was cut off. The round areas of SC were then dried on gaze, placed into extraction vials and finally dried over phosphorous dioxide in desiccator (overnight).

For the SC lipid analysis we used high performance thin layer chromatography (HPTLC) according to Bleck *et al.*⁶¹ The vials with samples were extracted in 2:1 chloroform–methanol (v/v) for 2 hours. Organic solutions were filtrated, then evaporated under stream of nitrogen and dried in desiccator.

The glass plate HPTLC (silica gel 60, Merck, Darmstadt, Germany) was cleaned with 2:1 chloroform–methanol (v/v), equilibrated and dried at 120°C for 30 min in a drying oven. on an HPTLC glass plate. The standards (calibration solutions) and samples (extracted from the tissue; concentration 200 µL/mg SC) as organic solutions (chloroform–methanol 2:1, v/v) were sprayed (30 µL) under a stream of nitrogen using Linomat 5 (Camag, Muttenz, Switzerland). The HPTLC plate was eluted two times with 95:4.5:0.75 chloroform–methanol–acetic acid

(v/v/v) in developing chamber (Camag, Muttenz, Switzerland). The dried plate was dipped in an aqueous solution of 10% CuSO₄, 8% H₃PO₄ (v/v), and 5% methanol for 10 s and then charred in a drying oven at 160°C for 30 min.⁵² After this procedure, the derived HPTLC plate was scanned by Scanner 3 (Camag, Muttenz, Switzerland).

3.6. Permeation Experiments

For the permeation experiment the Franz cells were used (see above). For my experiment, the Franz-type diffusion cells with an available diffusion area of 1.0 cm² (SC siding the donor compartment) and an acceptor volume 6.5±0.5 mL was used. The acceptor compartment of the cell was loaded with (PBS solution, pH = 7.4) and stirred at 32°C during the whole experiment. The exact volume for every individual cell was measured. Following a 12h equilibration at 32°C, the electric impedance and water loss were measured. Then, the donor samples (100 µL of either 5% theophylline (TH) or 2% indomethacin (IND) suspensions in 60% PG) were added onto the membrane (sample). During the permeation experiment, the acceptor phase (300 µL) were removed (via the shoulder) every 2 h over 8 h and were exchanged with the exact same volume of PBS.^{19, 21, 62}

3.7. Donor Samples for Permeation Studies

Donor samples for permeation studies were 2% (w/w) suspensions of IND in aqueous 60% PG (v/v) or 5% (w/w) suspensions of TH. The donor samples were mixed and re-suspended before the application on the SC. The concentration of IND/TH was chosen to make sure that all the donor samples were saturated with the model permeant in order to keep the exact thermodynamic activity for the whole experiment.^{52, 60, 63}

3.8. TEWL Measurement

Trans-epidermal water loss (TEWL) was measured in the Franz cells with their upper parts removed using an Aqua Flux AF 200 instrument (Biox Systems Ltd, UK) at 30–36% relative air humidity and 24–26°C. The Aqua Flux uses the condenser-chamber measurement method. The measured TEWL value is defined as the steady-state flux density of water diffusing through the membrane.^{64, 65}

3.9. Measurement of Electric Impedance

The electrical impedance was measured using LCR meter 4080 (Conrad Electronic, Hirschau, Germany; measuring range of 20 Ω to 10 M Ω , error at k Ω values less than 5%), which was controlled by the similar mode with an alternating frequency of 120 Hz. After adding 500 μ L of PBS at pH=7.4 in the donor compartment of each Franz cells (+ 1h equilibration), the electrical impedance was measured by immersing the tip of stainless steel probe into PBS in the acceptor compartments and donor of the Franz cells. Each cell was measured before the application of TH (IND) donor samples. After the measuring of electric impedance, the PBS was gently withdrawal from the donor compartment.^{52, 66}

3.10. High performance liquid chromatography (HPLC) of IND and TH

HPLC of IND and TH were calculated by isocratic reverse-phase using a Shimadzu Prominence instrument (Shimadzu, Kyoto, Japan) consisting of SIL-20A HT autosampler, CTO-20AC column oven LC-20AD pumps with a DGU-20A3 degasser, SPD20A diode array detector, and CBM-20A communication module. The data were examined using the LCsolutions 1.22 software. Acceptor phase sample for TH (20 μ L) was injected into the column, and the UV absorption of the effluent was measured at 272 nm, with a bandwidth of 4 nm. The retention time of TH was 3.2 \pm 0.1 min. Reverse phase separation of TH was achieved on a LiChroCART 250-4 column (LiChrospher 100 RP-18, 5 μ m, Merck, Darmstadt, Germany) at 35 $^{\circ}$ C, using 4:6 methanol/0.1 M NaH₂PO₄ (v/v) as a mobile phase at a flow rate of 1.2 mL/min. The IND samples were assayed on a LiChroCART 250-4 column (LiChrospher 100 RP-18, 5 μ m, Merck) using a mobile phase containing 90:60:5 acetonitrile/water/acetic acid (v/v/v) at a flow rate of 2 mL/min. After that, 100 μ L of acceptor phase was added into the column maintained at 40 $^{\circ}$ C.^{52, 67}

3.11. Evaluation of Permeation Data

Employing the Franz cells volumes and the measured concentration of TH and IND, the accumulative amount of TH and IND that penetrated over the SC membrane, was calculated. According to the cell volume, the cumulative amounts [μ g/cm²] of TH (IND) were corrected. From the amounts the steady state flux of TH and steady state flux IND [μ g/cm²/h] were calculated as a slope of the linear regression function obtained by fitting the linear region of the

plot in Excel. The resulted data are presented as the means \pm standard error of mean (SEM). For the analysis, the program GraphPad and unpaired t-test were used.

3.12. Fourier-Transform Infrared (FTIR) Spectroscopy

Fourier-transformed infrared spectroscopy (FTIR) is used to examine the lipid chain conformation and the performance of the polar headgroup region during the transition state and at skin temperature. Three types of samples were prepared: samples of SC without any application of solvents/1% solution of SPC, then samples with an addition of solvents (PG/EtOH), and finally the samples of SC with an addition of 1% solution of SPC. In my experiment, the FTIR spectra are controlled on a Nicolet 6700 spectrometer with ZnSe plate. The spectra were produced by the addition of 256 scans collected at 2 cm^{-1} resolution at laboratory temperature (PIKE technologies, Madison, WI). The precise peak location of any sample is decided from the second derivative spectra.

4. Results and Discussion

The main function of the skin, *i.e.*, the barrier function, is localized in the SC. In this work, we aimed to study the impact of Cer-precursor metabolite (*i.e.*, the SPC) on the SC permeability, integrity and microstructure. In many skin diseases, the amount of SPC is increased.⁵² However, there is not unclear if the presence of SPC increases or changes the SC structure and function. In this thesis we studied following markers/characteristics:

- permeability of SC (control samples: addition of PG/EtOH vs SPC samples: addition of 1% SPC in PG/EtOH) to water loss,
- permeability of SC to ions,
- permeability of SC to IND,
- permeability of SC to TH,
- chain order of lipids in SC, and
- amount of skin lipids in SC.

4.1. TEWL

First of all, we isolated the human SC from female patients according to the published procedures.⁶¹ Then performed the permeation experiments. In this experiment, I prepared two types of samples. First batch was the pure SC (control samples), on which only the mixture of solvents was applied. The second batch of samples were isolated SC pieces with applied solution of SPC in common used solvents. First, we measured the trans-epidermal water loss (TEWL).

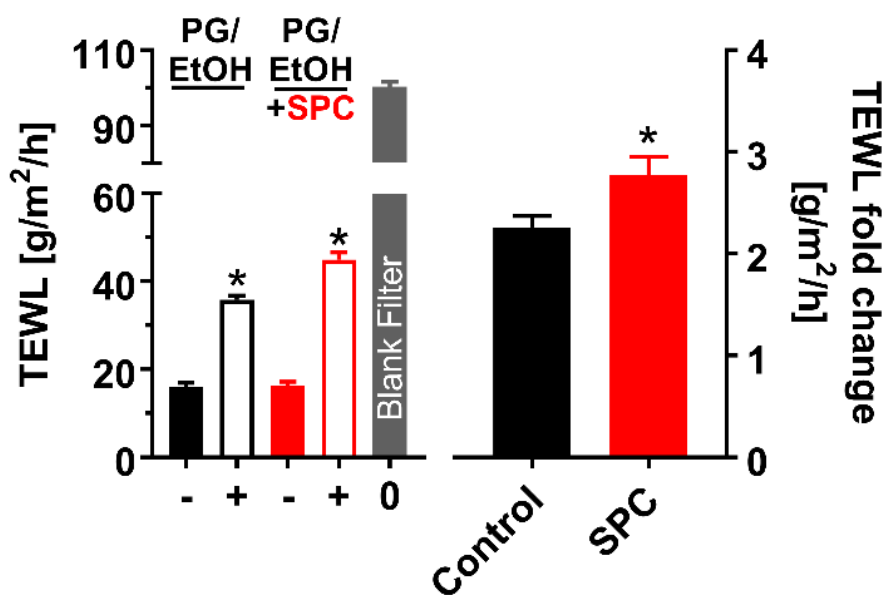


Figure 9. Effect of SPC on the SC permeability I. First graph describes the values of trans-epidermal water loss (TEWL) of control samples and SPC samples (black and red columns) before (filled columns) and after the solvent/1% SPC solution application (white-black and white-red columns). The TEWL of blank supporting filter (grey column) is also depicted. The second graph shows the TEWL fold change of control and SPC samples, calculated from the values from first graph. Data are presented as the means \pm standard error of mean (SEM), $n = 7-9$. *Statistically significant against controls.

This marker, a TEWL, is very important marker in dermatology, it is very often used in skin diseases diagnosis.⁶⁸⁻⁷⁰ As shown in **Figure 9**, first we measured the TEWL of all the samples before the application of either solvents or solution of SPC (black and red columns in first graph). The water loss of the control values was approximately 20 g/m²/h and these values were consistent. After the application of solvents/solution, the TEWL was measured again. The values of TEWL are depicted in first graph in **Figure 9**. On these samples, the TEWL fold change was calculated. The TEWL fold change of control samples was 2.26 \pm 0.11 g/m²/h, while the addition of SPC significantly increased the fold change (2.78 \pm 0.18 g/m²/h). Note: To confirm that the supporting filter does not have any effect on the TEWL, we also measured the TEWL of blank filters in Franz diffusion cells (“negative control”).

4.2. Electric Impedance

After the measuring of first permeability marker, the electric impedance was measured. Before the measuring with LCR meter,⁶⁶ on each sample 0.5 mL of PBS was applied. After the

equilibration, the electric impedance was measured. From this experiment we can see that the addition of either solvents or solution of SPC increases the permeability to ions. Electric impedance describes the resistance the tissue against the flux of ions. This parameter is also used for the membrane integrity investigation. The electric impedance of samples with solvents/1% SPC solution decreased (first graph in **Figure 10**). To confirm the minimal effect of the supporting filters on the permeability, the electric impedance of blank filter was measured (grey column in first graph of **Figure 10**). From the values, the electric impedance fold change was calculated (second graph in **Figure 10**). The control values reached the value 0.38 ± 0.05 g/m²/h, and the value for SPC 0.18 ± 0.02 g/m²/h, which was 2times less (significant) compared to controls. These results correlate with the TEWL. This confirms that the addition of SPC on the SC significantly increases the permeability of the tissue to water and ions.

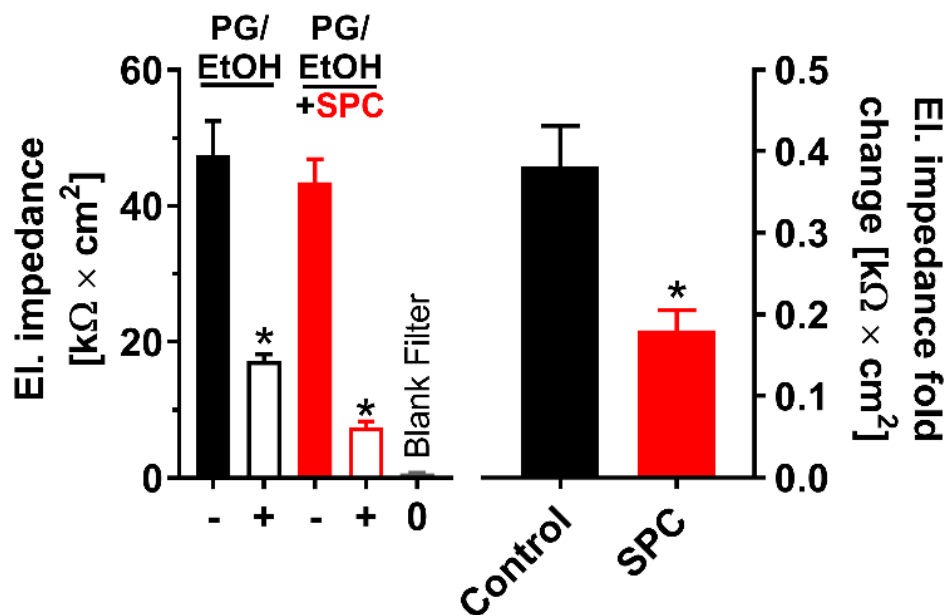


Figure 10. Effect of SPC on the SC permeability II. First graph describes the values of electric impedance of control samples and SPC samples (black and red column) before (filled columns) and after the solvent/SPC solution application (white-black and white-red columns). The electric impedance of blank supporting filter (grey column) is also depicted. The second graph shows the electric impedance fold change of control and SPC samples, calculated from the values from first graph. Data are presented as the means \pm standard error of mean (SEM), $n = 7-10$. *Statistically significant against controls.

4.3. Permeability to TH and IND

The third permeability marker we studied was the permeability to TH. TH is a typical small compound ($M_w = 180,164 \text{ g/mol}$) with a $\log P = -0.02$.⁶³ This substance represents a typical polar permeant with balanced lipophilicity. After the measuring of TEWL and electric impedance, a defined volume of 5% solution of TH was applied on each SC sample. We performed an 8h permeation experiment. After the mathematical correction in Excel, we prepared the permeation profile for TH. This profile (for control and SPC samples) is shown in **Figure 11** (first graph). The graph represents the amount of TH [μg], which penetrated across the defined diffusion area [cm^2] to acceptor compartment of Franz cell during the permeation experiment in time [h]. From the permeation profiles we calculated the flux of TH. This is shown in second graph of **Figure 11**. The flux of TH in the control samples was $1.95 \pm 1.06 \mu\text{g}/\text{cm}^2/\text{h}$. When we applied the lysolipid SPC on the SC, the permeability of the SPC samples to TH is higher in contrast to the control, *i.e.*, the flux was $6.08 \pm 1.97 \mu\text{g}/\text{cm}^2/\text{h}$, however without statistical differences. In addition, the flux of TH for the blank filter was $3269 \pm 174.8 \mu\text{g}/\text{cm}^2/\text{h}$. This again confirms the previous findings.

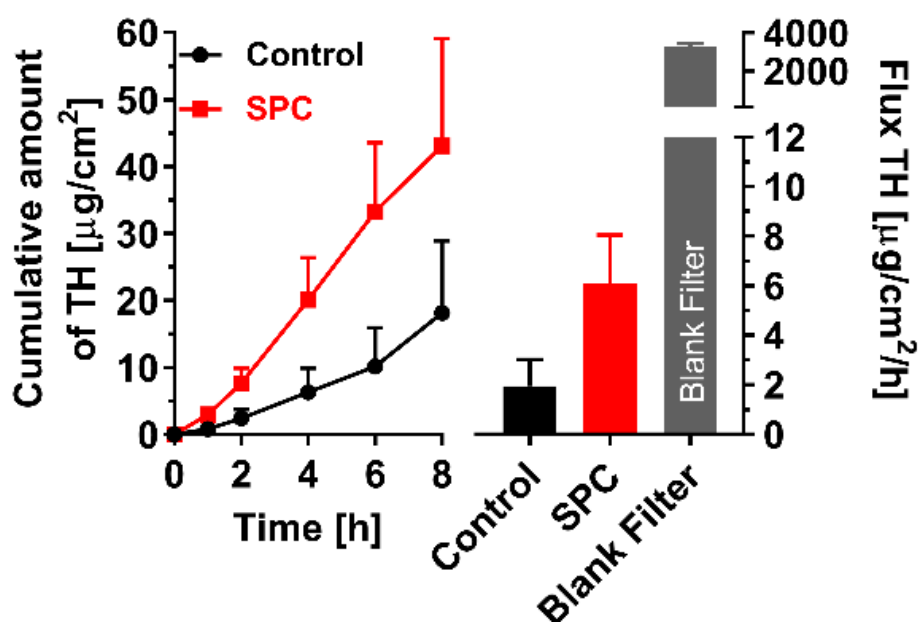


Figure 11. Effect of SPC on the SC permeability III. First graph describes the permeation profiles of TH (cumulative amount of TH) for control samples (black) and SPC samples (red) after the solvent/SPC solution application. The second graph shows the fluxes to TH for the control (black column), SPC samples (red column) and blank filters (grey column). Data are presented as the means \pm standard error of mean (SEM), $n = 9-11$.

The same experiment was then performed with second compound, with IND. This is a typical large ($M_w = 357.70$ g/mol) and lipophilic molecule ($\log P = 4.27$).⁶³ From the concentrations of IND (from HPLC), the cumulative amounts of IND were calculated (first graph in **Figure 12**) and from these we obtained the flux of IND (second graph in **Figure 12**). The flux of IND for the control samples was 0.61 ± 0.31 $\mu\text{g}/\text{cm}^2/\text{h}$, after the application of SPC on SC the flux increased (not significantly) to 2.01 ± 0.72 $\mu\text{g}/\text{cm}^2/\text{h}$. In addition, the flux of IND for the blank filter was determined, *i.e.*, 140.9 ± 43.66 $\mu\text{g}/\text{cm}^2/\text{h}$. In general, when the lysolipid SPC is applied onto the SC, the permeability to either TH or IND increased and this correlates to the TEWL and electric impedance.

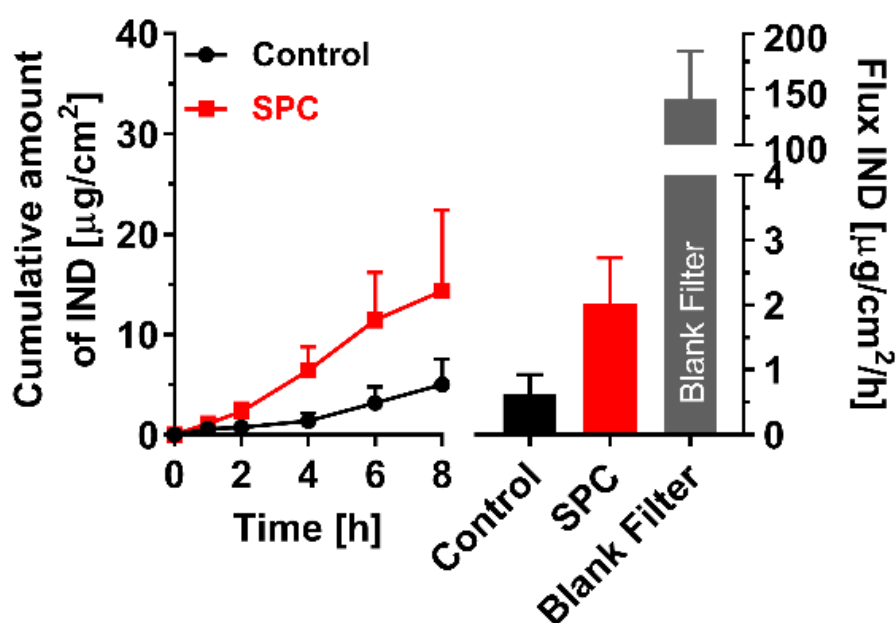


Figure 12. Effect of SPC on the SC permeability IV. First graph describes the permeation profiles of IND (cumulative amount of IND) for control samples (black) and SPC samples (red) after the solvent/SPC solution application. The second graph shows the fluxes to IND for the control (black column), SPC samples (red column) and blank filters (grey column). Data are presented as the means \pm standard error of mean (SEM), $n = 4-7$.

The main idea of this work was to investigate the role of polar lysolipids on the skin barrier permeability, *i.e.*, how the addition of SPC changes the permeability of SC to different permeants. Previously, Pullmannová *et al.*⁵² studied the role of SPC precursor, the SM. In this study, they prepared model membranes systems based on the sphingosine-Cer (CerNS)/isolated human Cer, Chol, FFA mixture and CholS. The model membranes were arranged by replacing

25, 50, 75 and 100 molar% of Cer (CerNS or isolated human Cer) with SM (from chicken egg; eSM). These skin barrier models were investigated by permeation experiments (TEWL, electric impedance, permeability to TH and permeability to IND). Pullmannová found out that the addition of SM in simple SC model membranes decreases the permeability to polar small and lipophilic large permeants, which was confirmed with decreasing TEWL and increasing resistance to flux of ions. This means that the Cer precursors lead to “better” permeability of model systems.

The second idea, why this thesis was performed is the confirmation of detrimental effect of SPC on the barrier permeability. Previously, one diploma thesis aimed to study the role in model SC membranes. In this study, model membranes based on isolated human Cer, FFA mixture, Chol, CholS with increasing amount of SPC (5, 10, 20, 50, and 100% replacement of Cer with SPC) were investigated (permeation and biophysical study). The results from our study confirm our hypothesis that the SPC partially increases the SC permeability, as shown in **Figures 9-12**.

4.4. FTIR Spectroscopy

To clarify the effect of SPC on the SC permeability, we prepared the SC samples for FTIR spectroscopy. This biophysical method is very accurate, with very good resolution.⁷¹⁻⁷⁴ For this experiment, three different sample types have been used. We prepared the SC samples in the same manner as for the permeation experiments, *i.e.*, the SC on which the mixture of solvents (PG/EtOH) was applied, then the SC samples with an addition of SPC. Additionally, we measured the SC without any addition of solvents/1% solution of SPC. Our model samples were incubated before the measuring at physiological temperature of 32°C in incubator overnight. From infrared spectra we studied the methylene symmetric stretching vibration (around 2850 cm⁻¹)⁷⁵ This vibration is very sensitive to lipid chain order (-CH₂- groups in skin lipid chains), and from this can be characterized several kinds of conformers.

In all the samples at physiological temperature (32°C), the skin lipids are well ordered, because the maxima of symmetric stretching did not reach the value 2850 cm⁻¹. As shown in **Figure 13A**, there is the clear trend (no significant differences) of detrimental effect of SPC on the lipid chain order. The healthy SC lipids (control sample) are well ordered (wavenumber 2848.59±0.12 cm⁻¹), so it means the chains are in all-*trans* conformation, which is important for the proper barrier function. However, samples with PG/EtOH or 1% SPC solution contain lipids, which are also well ordered, but the vibration is shifted to higher wavenumbers. In these

samples, the number of less ordered gauche conformers increased. From this experiment we can conclude that the SPC addition has as same negative effect (wavenumber $2849.13 \pm 0.27 \text{ cm}^{-1}$) as the addition of mixture of organic solvents (wavenumber $2849.59 \pm 0.15 \text{ cm}^{-1}$) used in this study. However, we can see some non-significant increase of chain disorder in SC with SPC. The representative spectra are shown in **Figure 13B**.

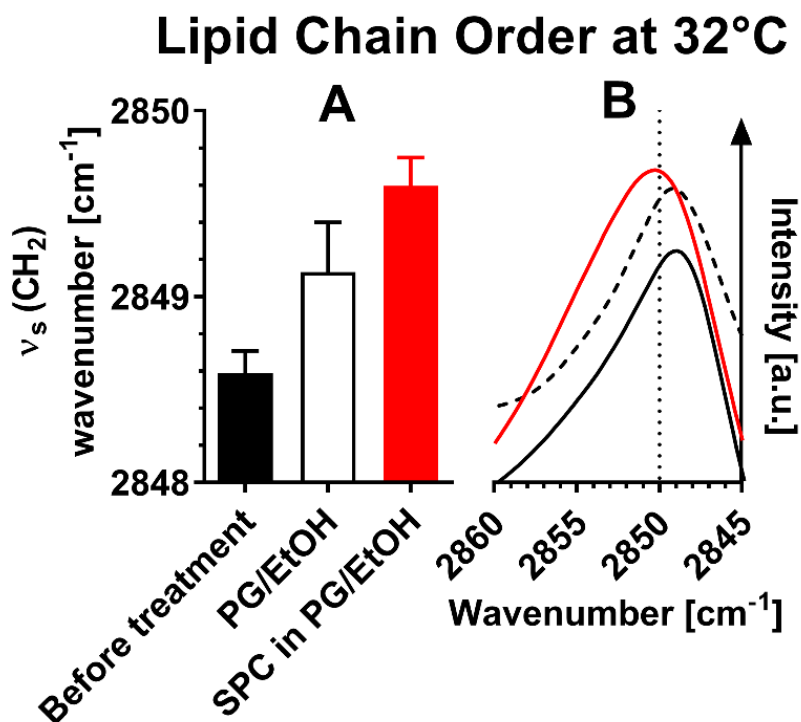


Figure 13. FTIR spectroscopy and lipid chain order of model SC samples at physiological temperature of 32°C . Panel A shows the symmetric stretching of SC before treatment (black column), and SC after the application of solvents (white column) and SC samples after the addition of SPC. Data are presented as the means \pm standard error of mean (SEM), $n = 4$. Panel B shows the representative FTIR spectra.

4.5. High Performance Thin Layer Chromatography

To clarify the effect of SPC on the SC microstructure and permeability, we simultaneously studied the amount (percentage) of lysolipid in our samples. We used the HPTLC technique, the method that is very often used in skin lipid analysis. First, we prepared the calibration solutions of skin lipids (FFA – the lignoceric acid was used, Chol, Cer – Cer EOS, Cer NS, Cer EOP, Cer NP, Cer AS and Cer AP were used). Then we applied the organic solution of extracted tissue. From the amount of SPC [$\mu\text{g SPC/mg SC}$] and sum of Cer [$\mu\text{g Cer/mg SC}$] we calculated

the SPC-Cer ratio. In this experiment, where 5 samples were quantified; we determined the SPC-Cer ratio = 0.196, *i.e.*, 16.6%.

5. Conclusions

In this work, we focused on the study of lysolipid effects on the skin permeability and microstructure. In many studies which describe the increase amounts of lysolipids in the human skin, is not clear if the presence of the lysolipids has negative effect on the barrier function. The aim of my work was to investigate one of the polar lysolipids, the SPC. This polar molecule is pathologically synthesized from the ceramide-precursor sphingomyelin.

First, in this study we had to isolate the human epidermis, then the *stratum corneum* and finally to prepare the samples for the permeation experiments. From the results we can conclude that the increased amounts of lysolipids (SPC in this case) have negative effect on the *stratum corneum* permeability. We observed some statistical differences in permeability to water and ions and trend in higher permeability to small polar and large lipophilic compounds. These changes in permeability were confirmed in infrared spectroscopy studies. We found out that the addition of SPC led to disorder of methylene chains of skin lipids.

In conclusion, this work confirmed some detrimental effects of lysolipids on the *stratum corneum* barrier function. This study supports some partial results from previous diploma thesis, *i.e.*, results from some permeability experiments with model *stratum corneum* membranes based on isolated skin ceramides with an addition of lysolipids. The work I performed could elucidate the role of lysolipids in some skin diseases (*e.g.*, atopic dermatitis) and could be helpful to clarify the understanding the lipid changes in skin pathology.

6. References

1. Williams, A., Transdermal and dermal drug delivery: From theory to clinical practice. London, Pharmaceutical Press. ISBN 0-85369-489-3: 2003.
2. Elias, P. M.; Friend, D. S., The permeability barrier in mammalian epidermis. *J Cell Biol* **1975**, *65* (1), 180-91.
3. Bouwstra, J. A.; Ponc, M., The skin barrier in healthy and diseased state. *Biochim. Biophys. Acta* **2006**, *1758* (12), 2080-95.
4. Eucerin.en, Structure and function of the skin. <http://www.eucerin.cz/o-kuzi/zakladni-informace/struktura-a-funkce-kuze> (online).
5. website, H. M., <https://www.webmd.com/skin-problems-and-treatments/picture-of-the-skin#1> (online).
6. Vávrová, K.; Kováčik, A.; Opálka, L., Ceramides in the skin barrier. **2017**, *64* (2), 28.
7. Novotný, J.; Hrabálek, A.; Vávrová, K., Synthesis and structure-activity relationships of skin ceramides. *Curr Med Chem* **2010**, *17* (21), 2301-24.
8. Breiden, B.; Sandhoff, K., The role of sphingolipid metabolism in cutaneous permeabilitybarrier formation. *Biochim. Biophys. Acta* **2014**, *1841* (3), 441-452.
9. van Smeden, J.; Janssens, M.; Gooris, G. S.; Bouwstra, J. A., The important role of stratum corneum lipids for the cutaneous barrier function. *Biochim. Biophys. Acta* **2014**, *1841* (3), 295-313.
10. Layers, T. S., <https://silkspace.wordpress.com/2016/10/25/the-5-skin-layers/> (online).
11. Elias, P. M.; Goerke, J.; Friend, D. S., Mammalian Epidermal Barrier Layer Lipids: Composition and Influence on Structure. *J. Invest. Dermatol.* **1977**, *69* (6), 535-546.
12. Elias, P. M., Epidermal lipids, membranes, and keratinization. *Int. J. Dermatol.* **1981**, *20* (1), 1-19.
13. Meckfessel, M. H.; Brandt, S., The structure, function, and importance of ceramides in skin and their use as therapeutic agents in skin-care products. *Journal of the American Academy of Dermatology* **2014**, *71* (1), 177-184.
14. Sochorová, M.; Audrlická, P.; Červená, M.; Kováčik, A.; Kopečná, M.; Opálka, L.; Pullmannová, P.; Vávrová, K., Permeability and microstructure of cholesterol-depleted skin lipid membranes and human stratum corneum. *J Colloid Interface Sci* **2019**, *535*, 227-238.
15. Shieh, H.-S.; Hoard, L. G.; Nordman, C. E., The structure of cholesterol. *Acta Crystallogr. Sect. B* **1981**, *37* (8), 1538-1543.

16. Norlen, L.; Nicander, I.; Lundsjo, A.; Cronholm, T.; Forslind, B., A new HPLC-based method for the quantitative analysis of inner stratum corneum lipids with special reference to the free fatty acid fraction. *Arch. Dermatol. Res.* **1998**, *290* (9), 508-16.
17. Kovacik, A.; Roh, J.; Vavrova, K., The chemistry and biology of 6-hydroxyceramide, the youngest member of the human sphingolipid family. *ChemBioChem.* **2014**, *15* (11), 1555-62.
18. Vávrová, K., Emerging small-molecule compounds for treatment of atopic dermatitis: a review. *Expert opinion on therapeutic patents* **2016**, *26* (1), 21-34.
19. Skolova, B.; Janusova, B.; Zbytovska, J.; Gooris, G.; Bouwstra, J.; Slepicka, P.; Berka, P.; Roh, J.; Palat, K.; Hrabalek, A.; Vavrova, K., Ceramides in the skin lipid membranes: length matters. *Langmuir : the ACS journal of surfaces and colloids* **2013**, *29* (50), 15624-33.
20. Skolova, B.; Jandovska, K.; Pullmannova, P.; Tesar, O.; Roh, J.; Hrabalek, A.; Vavrova, K., The role of the trans double bond in skin barrier sphingolipids: permeability and infrared spectroscopic study of model ceramide and dihydroceramide membranes. *Langmuir : the ACS journal of surfaces and colloids* **2014**, *30* (19), 5527-35.
21. Skolova, B.; Kovacik, A.; Tesar, O.; Opalka, L.; Vavrova, K., Phytosphingosine, sphingosine and dihydrosphingosine ceramides in model skin lipid membranes: permeability and biophysics. *BBA - Biomembranes* **2017**, *1859* (5), 824-834.
22. Kováčik, A.; Šílarová, M.; Pullmannová, P.; Maixner, J.; Vávrová, K., Effects of 6-Hydroxyceramides on the Thermotropic Phase Behavior and Permeability of Model Skin Lipid Membranes. *Langmuir : the ACS journal of surfaces and colloids* **2017**, *33* (11), 2890-2899.
23. Kota, V.; Hama, H., 2'-Hydroxy ceramide in membrane homeostasis and cell signaling. *Advances in biological regulation* **2014**, *54*, 223-30.
24. Rabionet, M.; Bayerle, A.; Marsching, C.; Jennemann, R.; Grone, H. J.; Yildiz, Y.; Wachten, D.; Shaw, W.; Shayman, J. A.; Sandhoff, R., 1-O-acylceramides are natural components of human and mouse epidermis. *J. Lipid Res.* **2013**, *54* (12), 3312-21.
25. Opálka, L.; Kováčik, A.; Maixner, J.; Vávrová, K., Omega-O-Acylceramides in Skin Lipid Membranes: Effects of Concentration, Sphingoid Base, and Model Complexity on Microstructure and Permeability. *Langmuir : the ACS journal of surfaces and colloids* **2016**, *32* (48), 12894-12904.
26. Hill, J.; Paslin, D.; Wertz, P. W., A new covalently bound ceramide from human stratum corneum -omega-hydroxyacylphytosphingosine. *International journal of cosmetic science* **2006**, *28* (3), 225-30.

27. Motta, S.; Monti, M.; Sesana, S.; Caputo, R.; Carelli, S.; Ghidoni, R., Ceramide composition of the psoriatic scale. *Biochim. Biophys. Acta* **1993**, *1182* (2), 147-51.
28. White, S. H.; Mirejovsky, D.; King, G. I., Structure of lamellar lipid domains and corneocyte envelopes of murine stratum corneum. An X-ray diffraction study. *Biochemistry* **1988**, *27* (10), 3725-32.
29. Elias, P. M.; Gruber, R.; Crumrine, D.; Menon, G.; Williams, M. L.; Wakefield, J. S.; Holleran, W. M.; Uchida, Y., Formation and functions of the corneocyte lipid envelope (CLE). *Biochim Biophys Acta* **2014**, *1841* (3), 314-318.
30. Banks-Schlegel, S.; Green, H., Involucrin synthesis and tissue assembly by keratinocytes in natural and cultured human epithelia. *J Cell Biol* **1981**, *90* (3), 732-7.
31. Mojumdar, E.; Gooris, G.; Groen, D.; Barlow, D. J.; Lawrence, M.; Demé, B.; Bouwstra, J., Stratum corneum lipid matrix: location of acyl ceramide and cholesterol in the unit cell of the long periodicity phase. *Biochimica et Biophysica Acta (BBA)-Biomembranes* **2016**, *1858* (8), 1926-1934.
32. Imokawa, G.; Ishida, K., Role of ceramide in the barrier function of the stratum corneum, implications for the pathogenesis of atopic dermatitis. *J Clin Exp Dermatol Res* **2014**, *5* (01), 1-12.
33. Rabionet, M.; Gorgas, K.; Sandhoff, R., Ceramide synthesis in the epidermis. *Biochim. Biophys. Acta* **2014**, *1841* (3), 422-434.
34. Mizutani, Y.; Mitsutake, S.; Tsuji, K.; Kihara, A.; Igarashi, Y., Ceramide biosynthesis in keratinocyte and its role in skin function. *Biochimie* **2009**, *91* (6), 784-90.
35. Levy, M.; Futerman, A. H., Mammalian ceramide synthases. *IUBMB Life* **2010**, *62* (5), 347-56.
36. Mizutani, Y.; Kihara, A.; Igarashi, Y., Identification of the human sphingolipid C4-hydroxylase, hDES2, and its up-regulation during keratinocyte differentiation. *FEBS Lett.* **2004**, *563* (1-3), 93-7.
37. de Jager, M. W.; Gooris, G. S.; Dolbnya, I. P.; Bras, W.; Ponec, M.; Bouwstra, J. A., Novel lipid mixtures based on synthetic ceramides reproduce the unique stratum corneum lipid organization. *Journal of lipid research* **2004**, *45* (5), 923-932.
38. de Jager, M.; Groenink, W.; Bielsa i Guivernau, R.; Andersson, E.; Angelova, N.; Ponec, M.; Bouwstra, J., A novel in vitro percutaneous penetration model: evaluation of barrier properties with p-aminobenzoic acid and two of its derivatives. *Pharm. Res.* **2006**, *23* (5), 951-60.

39. de Jager, M.; Gooris, G.; Ponec, M.; Bouwstra, J., Acylceramide head group architecture affects lipid organization in synthetic ceramide mixtures. *J. Invest. Dermatol.* **2004**, *123* (5), 911-6.
40. Hou, S. Y.; Mitra, A. K.; White, S. H.; Menon, G. K.; Ghadially, R.; Elias, P. M., Membrane structures in normal and essential fatty acid-deficient stratum corneum: characterization by ruthenium tetroxide staining and x-ray diffraction. *J. Invest. Dermatol.* **1991**, *96* (2), 215-23.
41. Madison, K. C.; Swartzendruber, D. C.; Wertz, P. W.; Downing, D. T., Presence of intact intercellular lipid lamellae in the upper layers of the stratum corneum. *J. Invest. Dermatol.* **1987**, *88* (6), 714-8.
42. Swartzendruber, D. C., Studies of epidermal lipids using electron microscopy. *Seminars in dermatology* **1992**, *11* (2), 157-61.
43. de Sousa Neto, D.; Gooris, G.; Bouwstra, J., Effect of the omega-acylceramides on the lipid organization of stratum corneum model membranes evaluated by X-ray diffraction and FTIR studies (Part I). *Chem. Phys. Lipids* **2011**, *164* (3), 184-95.
44. Bouwstra, J. A.; Gooris, G. S.; van der Spek, J. A.; Bras, W., Structural investigations of human stratum corneum by small-angle X-ray scattering. *J. Invest. Dermatol.* **1991**, *97* (6), 1005-12.
45. Bouwstra, J. A.; Gooris, G. S.; Bras, W.; Downing, D. T., Lipid organization in pig stratum corneum. *J. Lipid Res.* **1995**, *36* (4), 685-95.
46. Mojumdar, E. H.; Kariman, Z.; van Kerckhove, L.; Gooris, G. S.; Bouwstra, J. A., The role of ceramide chain length distribution on the barrier properties of the skin lipid membranes. *Biochim. Biophys. Acta* **2014**, *1838* (10), 2473-83.
47. Craven, B., Pseudosymmetry in cholesterol monohydrate. *Acta Crystallogr. Sect. B* **1979**, *35* (5), 1123-1128.
48. Norlen, L., Skin barrier structure and function: the single gel phase model. *J. Invest. Dermatol.* **2001**, *117* (4), 830-6.
49. Bouwstra, J. A.; Gooris, G. S.; Dubbelaar, F. E.; Ponec, M., Phase behavior of lipid mixtures based on human ceramides: coexistence of crystalline and liquid phases. *J. Lipid Res.* **2001**, *42* (11), 1759-70.
50. Damien, F.; Boncheva, M., The extent of orthorhombic lipid phases in the stratum corneum determines the barrier efficiency of human skin in vivo. *J. Invest. Dermatol.* **2010**, *130* (2), 611-4.

51. Mendelsohn, R.; Flach, C. R.; Moore, D. J., Determination of molecular conformation and permeation in skin via IR spectroscopy, microscopy, and imaging. *Biochim. Biophys. Acta* **2006**, *1758* (7), 923-33.
52. Pullmannová, P.; Staňková, K.; Pospíšilová, M.; Školová, B.; Zbytovská, J.; Vávrová, K., Effects of sphingomyelin/ceramide ratio on the permeability and microstructure of model stratum corneum lipid membranes. *Biochim. Biophys. Acta* **2014**, *1838* (8), 2115-26.
53. Okamoto, R.; Arikawa, J.; Ishibashi, M.; Kawashima, M.; Takagi, Y.; Imokawa, G., Sphingosylphosphorylcholine is upregulated in the stratum corneum of patients with atopic dermatitis. *Journal of lipid research* **2003**, *44* (1), 93-102.
54. Higuchi, K.; Kawashima, M.; Ichikawa, Y.; Imokawa, G., Sphingosylphosphorylcholine is a melanogenic stimulator for human melanocytes. *Pigment cell research* **2003**, *16* (6), 670-678.
55. Hara, J.; Higuchi, K.; Okamoto, R.; Kawashima, M.; Imokawa, G., High-Expression of Sphingomyelin Deacylase is an Important Determinant of Ceramide Deficiency Leading to Barrier Disruption in Atopic Dermatitis. *Journal of Investigative Dermatology* **2000**, *115* (3), 406-413.
56. Ishibashi, M.; Arikawa, J.; Okamoto, R.; Kawashima, M.; Takagi, Y.; Ohguchi, K.; Imokawa, G., Abnormal expression of the novel epidermal enzyme, glucosylceramide deacylase, and the accumulation of its enzymatic reaction product, glucosylsphingosine, in the skin of patients with atopic dermatitis. *Laboratory investigation* **2003**, *83* (3), 397.
57. Higuchi, K.; Junko, H.; OKAMOTO, R.; KAWASHIMA, M.; IMOKAWA, G., The skin of atopic dermatitis patients contains a novel enzyme, glucosylceramide sphingomyelin deacylase, which cleaves the N-acyl linkage of sphingomyelin and glucosylceramide. *Biochemical Journal* **2000**, *350* (3), 747-756.
58. Kim, H. J.; Kim, H.; Han, E.-S.; Park, S.-M.; Koh, J.-Y.; Kim, K.-M.; Noh, M.-S.; Kim, J.-J.; Lee, C.-H., Characterizations of sphingosylphosphorylcholine-induced scratching responses in ICR mice using naltrexon, capsaicin, ketotifen and Y-27632. *European journal of pharmacology* **2008**, *583* (1), 92-96.
59. KLIGMAN, A. M.; CHRISTOPHERS, E., Preparation of isolated sheets of human stratum corneum. *Archives of Dermatology* **1963**, *88* (6), 702-705.
60. Sochorová, M.; Staňková, K.; Pullmannová, P.; Kováčik, A.; Zbytovská, J.; Vávrová, K., Permeability Barrier and Microstructure of Skin Lipid Membrane Models of Impaired Glucosylceramide Processing. *Sci. Rep.* **2017**, *7* (1), 6470.

61. Bleck, O.; Abeck, D.; Ring, J.; Hoppe, U.; Vietzke, J. P.; Wolber, R.; Brandt, O.; Schreiner, V., *J. Invest. Dermatol.* **1999**, *113*, 894.
62. Pullmannová, P.; Pavlíková, L.; Kováčik, A.; Sochorová, M.; Školová, B.; Slepíčka, P.; Maixner, J.; Zbytovská, J.; Vávrová, K., Permeability and microstructure of model stratum corneum lipid membranes containing ceramides with long (C16) and very long (C24) acyl chains. *Biophys. Chem.* **2017**, *224*, 20-31.
63. Mitragotri, S., Modeling skin permeability to hydrophilic and hydrophobic solutes based on four permeation pathways. *J. Control. Release* **2003**, *86* (1), 69-92.
64. Stahlberg, S.; Eichner, A.; Sonnenberger, S.; Kováčik, A.; Lange, S.; Schmitt, T.; Demé, B.; Hauß, T.; Dobner, B.; Neubert, R. H. H.; Huster, D., Influence of a Novel Dimeric Ceramide Molecule on the Nanostructure and Thermotropic Phase Behavior of a Stratum Corneum Model Mixture. *Langmuir : the ACS journal of surfaces and colloids* **2017**, *33* (36), 9211-9221.
65. Kopečná, M.; Macháček, M.; Prchalová, E.; Štěpánek, P.; Drašar, P.; Kotora, M.; Vávrová, K., Dodecyl Amino Glucoside Enhances Transdermal and Topical Drug Delivery via Reversible Interaction with Skin Barrier Lipids. *Pharmaceutical research* **2017**, *34* (3), 640-653.
66. Fasano, W. J.; Hinderliter, P. M., The Tinsley LCR Databridge Model 6401 and electrical impedance measurements to evaluate skin integrity in vitro. *Toxicol. In Vitro* **2004**, *18* (5), 725-9.
67. Kováčik, A.; Pullmannová, P.; Maixner, J.; Vávrová, K., Effects of Ceramide and Dihydroceramide Stereochemistry at C-3 on the Phase Behavior and Permeability of Skin Lipid Membranes. *Langmuir : the ACS journal of surfaces and colloids* **2018**, *34* (1), 521-529.
68. Fokuhl, J.; Müller-Goymann, C. C., Modified TEWL in vitro measurements on transdermal patches with different additives with regard to water vapour permeability kinetics. *Int. J. Pharm.* **2013**, *444* (1-2), 89-95.
69. De Paepe, K.; Houben, E.; Adam, R.; Wiesemann, F.; Rogiers, V., Validation of the VapoMeter, a closed unventilated chamber system to assess transepidermal water loss vs. the open chamber Tewameter. *Skin research and technology : official journal of International Society for Bioengineering and the Skin (ISBS) [and] International Society for Digital Imaging of Skin (ISDIS) [and] International Society for Skin Imaging (ISSI)* **2005**, *11* (1), 61-9.
70. Netzlaff, F.; Kostka, K.-H.; Lehr, C.-M.; Schaefer, U. F., TEWL measurements as a routine method for evaluating the integrity of epidermis sheets in static Franz type diffusion

cells in vitro. Limitations shown by transport data testing. *Eur. J. Pharm. Biopharm.* **2006**, *63* (1), 44-50.

71. Moore, D. J.; Rerek, M. E.; Mendelsohn, R. J. T. J. o. P. C. B., FTIR spectroscopy studies of the conformational order and phase behavior of ceramides. **1997**, *101* (44), 8933-8940.

72. Moore, D. J.; Rerek, M. E.; Mendelsohn, R., Lipid domains and orthorhombic phases in model stratum corneum: evidence from Fourier transform infrared spectroscopy studies. *Biochemical and biophysical research communications* **1997**, *231* (3), 797-801.

73. Boncheva, M.; Damien, F.; Normand, V., Molecular organization of the lipid matrix in intact Stratum corneum using ATR-FTIR spectroscopy. *BBA - Biomembranes* **2008**, *1778* (5), 1344-1355.

74. Rerek, M. E.; Van Wyck, D.; Mendelsohn, R.; Moore, D. J., FTIR spectroscopic studies of lipid dynamics in phytosphingosine ceramide models of the stratum corneum lipid matrix. *Chem. Phys. Lipids* **2005**, *134* (1), 51-58.

75. Mendelsohn, R.; Moore, D. J., Vibrational spectroscopic studies of lipid domains in biomembranes and model systems. *Chem. Phys. Lipids* **1998**, *96* (1-2), 141-57.